Minimum Pressure Coefficient Criterion Applied in Axial-Flow Hydraulic Turbines

Antonio Guilherme B. da Cruz
agcb@ufpa.br
Federal University of Pará - UFPA
Faculty of Mechanical Engineering
66075-110 Belém, PA, Brazil

André Luiz A. Mesquita
andream@ufpa.br
Federal University of Pará - UFPA
Faculty of Mechanical Engineering
66075-110 Belém, PA, Brazil

Cláudio José C. Blanco
blanco@ufpa.br
Federal University of Pará - UFPA
Faculty of Sanitary Environmental Engineering
66075-110 Belém, PA, Brazil

The recent development of computer-based tools with more efficient algorithms has allowed a substantial improvement in hydraulic turbine design. The definition of an initial geometry capable to assist certain characteristics of turbine performance is a first step for useful numerical turbine analysis. This paper presents an application of the minimum pressure coefficient criterion for axial-flow hydraulic turbines cascade geometry design. In recent works, the criterion was tested for axial fan and it was showed that it is suitable to define the initial geometry for machine design. The global parameters that supply the principal dimensions of the turbine are obtained from the literature as based upon statistical data of installed power plants. The grid of the simulation domain was generated with CFX-TURBO grid software package and the results were obtained using the commercial package Navier-Stokes 3-D CFX-TASCflow to analyze the fluid flow through blade runner. Using this procedure, a study was carried out on a small axial-flow turbine, specifically designed to operate in a small river in the Amazon region. An interpretation of the flow through the turbine's hydraulic channels is presented for nominal flow rate operation points. Finally, the results are evaluated to hydraulic efficiency prediction of blade runner turbines
Keywords*: axial-flow turbine, axial cascade, small hydro turbine design, turbine impeller*

Introduction

The development of methodologies for the hydraulic turbines design with high efficiency and that assure the hydraulic characteristics sought in the design has been of great importance. The increasing development of numeric tools with more efficient algorithms, evidenced by the recent development of computational fluid dynamics (CFD) and the advent of faster numeric processors, has allowed the treatment of complex flows found in turbomachinery (De Palma, 2006; Nilsson and Davidson, 2003). The ability to predict three-dimensional viscous flow within the passages of rotating machinery devices is of considerable interest to the industry. A CFD analysis provides a complementary effective cost, but still can serve to reduce the amount of component testing required. However, at the initial stage of the turbomachinery design, there is a lack of information on the necessary geometrical definition for advanced CFD code application. At this stage of the design, it is necessary to employ some design criteria aiming at assuring certain performance requirements, such as optimal operational parameters, aerodynamic loading, cavitation, shock effects, stall limits, etc.

In that sense, some studies present a good review of various aerodynamic performance criteria for axial flow cascades of turbomachinery. De La Fuente (1982) has employed the experimental data of Herrig et al. (1957) for NACA 65-series-airfoil cascades. This work confirms the use of the criterion of the minimum suction pressure coefficient in the evaluation of the optimum conditions of operation axial cascades with minimum aerodynamic loss. Initially, this criterion was idealized by Scholz (1965) for isolated airfoils and later it was tested (Fernandes, 1973) in axial flow pumps. The criterion was also tested by Amarante Mesquita et al. (1996, 1999) in the selection of minimum aerodynamic loss cascade for axial fan, showing good results. It was also used for definition of the initial geometry of turbomachines. Nevertheless, more studies are necessary in order to evaluate the real applicability of this criterion in axial-flow hydraulic turbine design.

Simplified methodologies that provide a complete axial hydraulic turbine design are scarce and hardly available in the literature. Thus, this paper presents an application of the minimum pressure coefficient criterion for axial-flow hydraulic turbines design. The criterion is used in the selection of good aerodynamic performance cascade for the initial geometry definition of the runner blades. The cascade panel method is used to compute pressure distribution around the runner. In this inviscid method, a correction is applied for accounting the boundary layer effect on the cascade deflection angle, following the Gostelow procedure (Gostelow, 1974; Manzanares Filho, 1994).

In order to verify the applicability of the methodology under consideration, five axial hydraulic turbines were designed to evaluate the optimum minimum suction pressure coefficient value suitable for cascade design turbines. The turbines were designed from real data of a small river of the Amazon (Cruz, 2002). The global parameters of the turbines are determined from statistical correlations available in the literature (Schweiger and Gregori, 1990). CFX-TURBOgrid software package, specific to work with geometries of turbomachinery, was used to generate the grid of the simulation domain. The analysis of the turbine's quality geometries was conducted using the commercial package Navier-Stokes 3-D CFX-TASCflow (AEA, 2000), specific for solution of turbo-machinery flows. The results are evaluated for the prediction of hydraulic efficiencies, search for an optimum value of the minimum suction pressure coefficient design criteria for this turbine type. Based on this prediction, a range was proposed for the minimum suction pressure coefficient, C_{psmin}, for small axial hydraulic turbines design with high efficiency. Also, flow visualization was presented through the blade channels. Finally, an analysis discussing the different values of C_{psmin} is proposed for turbine design and the previous values set for fan design is presented.

Paper accepted May, 2007. Technical Editor: Francisco R. Cunha.

Nomenclature

$\vec{c}$ = *absolute velocity, m/s*
C_D = *drag coefficient, related to the mean velocity, dimensionless*
C_L = *lift coefficient, dimensionless*
C_{psmin} = *minimum suction pressure coefficient, dimensionless*
C_p = *pressure coefficient, dimensionless*
C_b = *camber coefficient, dimensionless*
c_r = *radial velocity component, m/s*
c_m = *meridian velocity, m/s*
D = *runner diameter, m*
E = *specific energy, J/kg*
H = *head, m*
l = *chord of profile, m*
l/s = *solidity of profile, dimensionless*
n = *rotational speed, rpm*
n_q = *specific speed, dimensionless*
P = *power, W*
p = *static pressure on the blade profile, Pa*
P_h = *hydraulic power, W*
P_u = *shift power, W*
p_o = *reference pressure, Pa*
p_3 = *inlet static pressure, Pa*
p_4 = *outlet static pressure, Pa*
Q = *flow rate, m^3/s*
R = *radius, m*
s = *distance between the airfoil cascade, m*
T = *torque, N·m*
$\vec{u}$ = *rotation velocity, m/s*
$\vec{w}$ = *relative velocity, m/s*
w_a = *axial velocity component, m/s*
$\vec{w}_3$ = *inlet relative velocity, m/s*
$\vec{w}_4$ = *outlet relative velocity, m/s*
$\vec{w}_\infty$ = *mean relative velocity, m/s*

Greek Symbols

Δp_o = loss stagnation pressure, Pa
Δc_u = difference between the tangential velocity components, m/s
α = angle of attack in relation to $\vec{w}_\infty$, degree
α_3 = angle of attack in relation to $\vec{w}_3$, degree
β = stagger angle, degree
β_3 = inlet flow angle, degree
β_4 = outlet flow angle, degree
β_∞ = mean angle of flow velocity, degree
$\Delta\beta$ = cascade deflection angle, degree
ΔW_u = difference between the tangential velocity components, m/s
δ_u = cascade deflection coefficient, dimensionless
ζ_v = loss coefficient, dimensionless
η = efficiency, dimensionless
φ = flow number, dimensionless
λ = hydraulic power number, dimensionless
ν = velocity coefficient, dimensionless
ρ = fluid density, kg/m^3
σ = cascade solidity, dimensionless
τ = torque number, dimensionless
ϑ = specific diameter, dimensionless
ω = angular velocity, rad/s
ψ = pressure coefficient number, dimensionless

Subscripts

e = relative to the external region of the turbine
i = relative to the internal region of the turbine
m = relative to the meridian direction
u = relative to the tangential direction
∞ = relative to the mean direction of the flow
3 = relative to the inlet of the cascade
4 = relative to the outlet of the cascade

Turbine Cascade Geometry and Hydrodynamic Coefficients

In general, the analysis of flow through two-dimensional turbine cascade considers the radial velocity component as being null; with the current surfaces remaining cylindrical and parallel to the rotation axis. This condition is possible if the meridian velocity remains constant.

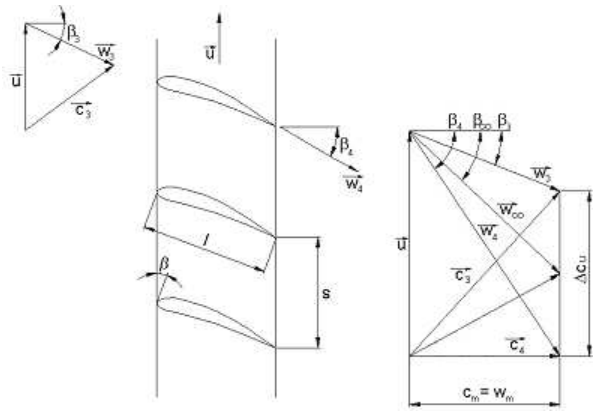

Figure 1. The cascade geometry and velocity triangles.

Figure 1 presents a two-dimensional cascade geometry of a turbine, which performs the required flow deflection, together with the corresponding velocity triangles, where $\vec{c}$ is the absolute velocity and $\vec{w}$ is the relative velocity. The cascade moves with velocity $\vec{u}$. The cascade deflection angle is defined as

$$\Delta\beta = \beta_4 - \beta_3 \tag{1}$$

The angles β_3 and β_4 define the direction of the inlet $\vec{w}_3$ and outlet $\vec{w}_4$ flow velocity taken in relation to axial direction of the flow, respectively. Observing the geometric relationships, it is verified the following relationships between the angles of the flow and of the cascade

$$\beta_3 = \beta - \alpha_3 \tag{2}$$

$$\beta = \beta_\infty + \alpha \tag{3}$$

where β is the stagger angle, β_∞ is the mean angle that define the direction of mean flow velocity, α_3 and α are the angles of attack taken in relation to $\vec{w}_3$ and $\vec{w}_\infty$ velocities, respectively. The deflection angle can also be expressed by the dimensionless cascade coefficient δ_u, defined as

$$\delta_u = \frac{\Delta W_u}{W_a} = \tan\beta_3 - \tan\beta_4 \tag{4}$$

where ΔW_u is the difference between the tangential velocity components and W_a is the axial velocity component.

The flow is considered as two-dimensional, incompressible, isothermal, and in steady-state condition. The application of the momentum equation in both axial and tangential directions one can obtain the following expression

$$C_L \cdot \sigma = \zeta_v \cos^2 \beta_\infty \cdot \sin \beta_\infty - 2 \cdot \delta_u \cdot \cos \beta_\infty \tag{5}$$

$$C_D \cdot \sigma = \zeta_v \cos^3 \beta_\infty \tag{6}$$

where C_D is the drag coefficient, C_L the lift coefficient, β_∞ is the angle between the mean velocity and the axial direction; $\vec{w}_\infty$ is defined by

$$\vec{w}_\infty = \frac{\vec{w}_3 + \vec{w}_4}{2} \tag{7}$$

σ is the cascade solidity, relationship between the blade chord l and the step s (distance between a blade and other adjacent one), and ζ_v is the dimensionless loss coefficient of the cascade defined by

$$\zeta_v = \frac{\Delta p_o}{\frac{1}{2}\rho W_a^2} \tag{8}$$

$$\Delta p_o = \left(p_3 + \frac{1}{2}\rho W_3^2 \right) - \left(p_4 + \frac{1}{2}\rho W_4^2 \right) \tag{9}$$

Δp_o represents the global loss of the stagnation pressure through the cascade; p_3 and p_4 are the inlet and outlet static pressures, respectively. For inviscid flow, $C_D = 0$, consequently, $\zeta_v = 0$ and the Eq. (5) reduces to

$$C_L \cdot \sigma = 2 \frac{\Delta W_u}{W_a} \tag{10}$$

Equations (5-6) relate the coefficient of loss, the deflection coefficient, the inflow angle and the cascade parameters (solidity, stagger angle and profile geometry). Equation (10) is the classical relation employed in the turbomachinery design, which can be also derived from the Kutta-Joukowsky theorem. The term $C_L \ \sigma$ is associated with the constructive characteristics of the turbomachinery, which should be quite defined by the cascade that can reproduce the characteristics of the desired flow. The term $\Delta W_u / W_a$ is associated with the characteristics of the flow.

The Minimum Suction Pressure Coefficient Criterion

The pressure coefficient is an important parameter and gives information on the aerodynamic loading of de cascade blades. It is defined as

$$C_p = \frac{p - p_o}{\frac{1}{2}\rho W_\infty^2} \tag{11}$$

where p is the static pressure on the blade profile and p_o is a reference pressure.

The minimum suction pressure coefficient C_{psmin} is defined as the minimum value of the pressure coefficient on the airfoil suction side. Normally, p_o is the upstream static pressure, and this gives a negative value for C_{psmin}. This coefficient can be used as an aerodynamic loading criterion, allowing the selection of cascade with relatively low profile losses. Figure 2 illustrates this concept. There is a C_{psmin} interval limited by a lower value, C_{psi}, and a higher value, C_{pss}, which corresponds to a cascade with a low coefficient of loss. It is important to note that both C_{psi} and C_{pss}, have negative values. For $C_{psmin} > C_{pss}$, a slightly load is obtained, and the danger of the boundary layer separation is reduced, but a comparatively large area is exposed to the flow, i.e., the friction losses are augmented. In contrast, for a cascade with $C_{psmin} < C_{psi}$, the frictional area is relatively small but a comparatively high pressure loading is observed, increasing the danger of separation. So, in order to apply this criterion it is essential to determine the $C_{psi} < C_{psmin} < C_{pss}$ interval. A suitable way to accomplish this task is to test a series of turbomachines especially designed for this purpose.

Inviscid Method Calculation

The minimum suction pressure coefficient criterion is established by potential flow calculation through a panel method (Manzanares Filho, 1994; Amorim, 1986). The numeric technique involves the representation of the flow by distributed voricitty sheet clothing the whole blade profile. The resulting boundary integral equation is solved through a computational scheme proposed by Lewis (1991). In order to provide the deflection angle with an acceptable value, an empirical correction is employed to take into account the viscous effects. This correction was proposed by Gostelow (1974) and consists in fairing-in the pressure distribution to avoid non-natural strong pressure gradients at the trailing edge region with tangential extrapolation of the pressure curves on both blade profile sides. Larger details of this procedure can be found in Manzanares Filho (1994).

Global Turbine Parameters and Hydraulic Numbers

A hydraulic turbine is characterized by the specific speed, n_q, usually expressed by the equation

$$n_q = n \cdot \frac{\sqrt{Q}}{H^{0.75}} \tag{12}$$

that determines the type and the basic geometry of the runner, as well as other components of the turbomachinery. Notice that n is the rotating velocity; Q and H are the flow rate and the available head, respectively.

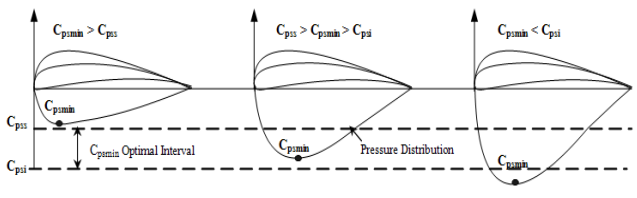

Figure 2. The minimum suction pressure coefficient criterion concept.

The appropriate specification of the specific speed is important because the global parameters of the turbine are directly related to that value. It also defines the applicability domain and comparison means between the different types of hydraulic turbines.

The global parameters of the turbine, normally presented in dimensionless form, define the operation characteristics of the turbines describing its behavior in several operational conditions.

Therefore, considering a hydraulic turbine within an available head H, angular velocity ω, flow rate Q and specific energy E, the turbine operation point is defined for the following parameters,

flow number,

$$\varphi_e = \frac{Q}{\pi \cdot \omega \cdot R_e^{\,3}} \tag{13}$$

pressure coefficient number,

$$\psi_e = \frac{2 \cdot E}{\omega^2 \cdot R_e^2} \tag{14}$$

specific diameter,

$$\vartheta_e = \frac{\psi_e^{0.25}}{\varphi_e^{0.5}} \tag{15}$$

$$\vartheta_e = \frac{\pi^{0.5} \cdot D_e \cdot E^{0.25}}{2^{0.75} \cdot Q^{0.5}} \tag{16}$$

hydraulic power number,

$$\lambda_e = \frac{2 \cdot \rho \cdot E \cdot Q}{\pi \cdot \rho \cdot \omega^3 \cdot R_e^5} \tag{17}$$

$$\lambda_e = \varphi_e \cdot \psi_e \tag{18}$$

torque number,

$$\tau_e = \frac{2 \cdot T}{\pi \cdot \rho \cdot \omega^2 \cdot R_e^5} \tag{19}$$

$$\tau_e = \varphi_e \cdot \psi_e \cdot \eta \tag{20}$$

efficiency,

$$\eta = \frac{\tau_e}{\lambda_e} \tag{21}$$

velocity coefficient,

$$\nu = \frac{\varphi_e^{0.5}}{\psi_e^{0.75}} \tag{22}$$

where ρ is the fluid density, R_e is the external radius of de runner, D_e is the external diameter and T the blade torque.

Small Axial Turbines Design

The axial hydraulic turbines present as characteristic a high specific speed, being advantageous for hydroelectric projects in sites with low head and high flows rate. For this turbine type, it is necessary to test the minimum suction pressure coefficient criterion for turbine cascade design. Thus, five axial hydraulic turbines were designed. The turbine parameters were obtained from the studies of Schweiger and Gregori (1990), which propose correlations based in statistical data collected from existing plants, various specialized manufacturers and other sources. Those correlations furnish the hydraulic, energy and the main geometric small turbine parameters. Thus, the blade design can be performed according to some criteria and simplifications can be introduced without affecting the efficiency very much.

Equations (23-25) present the regression characteristic functions linking the head and specific speed, $H = f(n_q)$, in relation to the corresponding power range (Schweiger and Gregori, 1990):

1MW < P < 2MW,

$$H = 455.000 \cdot n_q^{\,-2} \tag{23}$$

0.5MW < P < 1MW,

$$H = 355.000 \cdot n_q^{\,-2} \tag{24}$$

P < 0.5MW,

$$H = 255.000 \cdot n_q^{\,-2} \tag{25}$$

where H is the available head, n_q the specific speed and P the power. Also, the flow number, pressure coefficient number and specific diameter are presented as function of the specific speed $\psi = f(n_q)$, $\varphi = f(n_q)$ and $\vartheta = f(n_q)$, respectively. Thus, the following regression functions can be established:

$$\varphi = 0.162 + 7.8 \cdot 10^{-4} \cdot n_q \tag{26}$$

$$\psi = 26.1 \cdot n_q^{\,-0.85} \tag{27}$$

$$\vartheta = 1.636 \cdot n_q^{\,-0.5} \tag{28}$$

The corresponding runner diameter can be obtained with the re-arranging Eq. (16)

$$D_e = \frac{2^{0.75} \cdot \vartheta \cdot Q^{0.5}}{\pi^{0.5} \cdot E^{0.25}} \tag{29}$$

Table 1 presents the nominal conditions of project and the dimensionless parameters obtained by Eq. (25-29). They have been calculated with the nominal values for the flow rate (Q = 1.8 m^3/s) and head (H = 3 m), which were collected from a small river in the Amazon region. The external diameter was obtained by Eq. (29) and the internal diameter was established from procedures, as indicates in the literature (Raab, 1985). The cascade designs for the blade radial stations were made assuming the free-vortex radial equilibrium condition. This flow distribution results in a constant axial velocity component and also in a uniform radial distribution of the specific energy and, consequently, in highly twisted blades.

Table 1. Nominal conditions for the turbine design.

Hydraulic power, P_h [kW]	57,97
Hydraulic efficiency, η_h [-]	0,900
Hydraulic global, η_g [-]	0,850
Shift power estimated, P_u [kW]	49,28
Specific energy, E [J/kg]	32,21
Theoretical specific energy, $E_{pá}$ [J/kg]	28,99
Rotational speed, n [rpm]	506,6
Specific speed, n_q [-]	278,7
Pressure coefficient number, ψ_e [-]	0,218
Flow number, φ_e [-]	0,296
Specific diameter, ϑ_e [-]	1,253
External diameter, D_e [m]	0,669
Internal diameter, D_i [m]	0,307

Table 2 shows the main cascade design data for radial stations (Fig. 3); the absolute velocity and the relative flow angles obtained through the velocity triangles at the inlet and outlet blade sections. In this table, the $C_L \cdot \sigma$ value was evaluated by Eq. (10).

Table 2. Cascade design data of the radial stations.

Radial Stations	i	1	2	3	e
D [m]	0,307	0,397	0,488	0,579	0,669
S [m]	0,241	0,312	0,383	0,455	0,526
U [m/s]	8,134	10,541	12,947	15,354	17,760
Δc_u [m/s]	3,563	2,750	2,239	1,888	1,632
W∝ [m/s]	9,314	11,419	13,649	15,938	18,262
W_3 [m/s]	8,203	10,348	12,691	15,090	17,507
β∝ [degree]	43,004	53,384	60,064	64,701	68,101
β_3 [degree]	33,864	48,838	57,542	63,169	67,105
β_4 [degree]	50,059	57,131	62,253	66,077	69,018
C_L σ [-]	0,765	0,482	0,328	0,237	0,179

Analysis of the Minimum Pressure Coefficient Criterion

In the application of the minimum suction pressure coefficient criterion for flow design through turbomachinery cascade, it is possible to find a set of cascades that can satisfy both the minimum suction pressure coefficient criterion and the required aerodynamic conditions (Manzanares Filho, 1994). With a specific airfoil profile, the defined geometrical parameters of the cascade for (β, σ), are computed in order to satisfy both the cinematic condition (for instance the deflection angle, Δβ) and a required value for C_{psmin}. However, it is possible to adopt a new profile and then determine a new set of parameters (β, σ), which satisfies the same conditions for $\Delta\beta$ and C_{psmin}. Thus, one obtains a family of design solutions, and for this reason the C_{psmin} criterion cannot be employed alone, but in conjunction with a loss prediction method. The design must be refined in order to select the optimal cascade in this family.

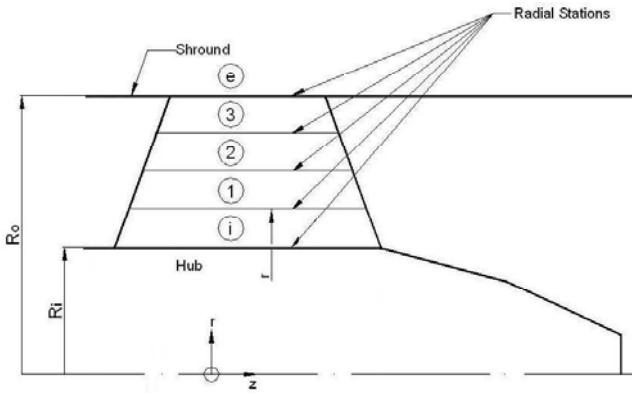

Figure 3. Blade Runner radial stations.

For the evaluation of C_{psmin} as criterion of turbine cascade design, the NACA 65-(C_b)10 (C_b is the camber coefficient) profiles were adopted. A set of cascades was designed for each radial station (Fig. 3). For each cascade design the geometrical values were determined in relation to the flow angles and the hydrodynamic conditions. Table 3 shows the cascade family according to the design parameters and matching a minimum suction pressure coefficient.

Normally, in runner design of axial hydraulic turbines the blade chord length assumes the smallest value in the inner radial station (station close to the hub) due to the limit the stall effects. Also, by using empirical rules the radial distribution of the solidity is given as a function of the specific speed, in order to prevent cavitation (Raab, 1985). Since the cavitation index is related with the C_{psmin} the cavitation danger appears when the minimum pressure is equaled with the vapor pressure, meaning that the cavitation index is equaled to the C_{psmin} value. Thus, the range of C_{psmin} should be such that the cavitation danger does not occur.

Therefore, once the nominal condition imposes the design of a turbine with specific speed equal to 278.7 and from an appropriate interpolation, the value of the solidity close to the hub station was determined as being equal to 1.210, and in the more external radial station equal to 0.730. The solidity and, consequently, the profile chord lengths l of the intermediate radial station profiles were obtained so that, in horizontal projection, both edges of the blade have an approximately linear form. The cascade solidity value decreases from the hub to the tip of the blade in order the chord length at tip blade is outside the risk of cavitation. This implicates in fine blade profiles with low curvature or with small values of solidity as well as in a few blade runner (Raab, 1985).

Table 3. Cascades Designs.

Radial Station i – σ = 1.21, β_3 = 33.864, β_∞ = 43.004, Δβ = 16.195, C_L = 0.632						
C_b	Cp_{min}	l	α_3	β	$\Delta\beta_{pot}$	C_{Lpot}
0.1	-4.246	0.292	13.29	47.154	16.192	0.632
0.2	-3.208	0.292	12.520	46.384	16.192	0.632
0.3	-0.712	0.292	11.555	45.415	1.192	0.632
0.4	-0.712	0.292	10.737	44.601	16.192	0.632
0.5	-0.713	0.292	9.918	43.782	16.192	0.632
0.8	-0.723	0.292	7.468	41.332	16.192	0.632
1.0	-0.733	0.292	5.848	39.712	16.192	0.632
1.2	-0.752	0.292	4.251	38.115	16.192	0.632
Radial Station 1 – σ = 1.0, β_3 = 48.838, β_∞ = 53.384, Δβ = 8.293, C_L = 0.482.						
C_b	Cp_{min}	l	α_3	β	$\Delta\beta_{pot}$	C_{Lpot}
0.1	-0.556	0.312	5.822	54.660	8.297	0.482
0.2	-0.562	0.312	5.114	53.952	8.297	0.482
0.3	-0.571	0.312	4.401	53.239	8.297	0.482
0.4	-0.580	0.312	3.685	52.523	8.297	0.482
0.5	-0.588	0.312	2.967	51.805	8.297	0.482
0.8	-0.620	0.312	0.810	49.648	8.297	0.482
Radial Station 2 – σ = 0.87, β_3 = 57.542, β_∞ = 60.064, Δβ = 4.711, C_L = 0.377						
C_b	Cp_{min}	l	α_3	β	$\Delta\beta_{pot}$	C_{Lpot}
0.1	-0.473	0.333	2.823	60.365	4.710	0.377
0.2	-0.485	0.333	2.178	59.720	1.710	0.377
0.3	-0.499	0.333	1.528	59.070	4.710	0.377
0.4	-0.512	0.333	0.875	58.417	4.710	0.377
0.5	-0.524	0.333	0.219	57.761	4.710	0.377
Radial Station 3 – σ = 0.800, β_3 = 63.169, β_∞ = 64.701, Δβ=2.908, C_L = 0.296						
C_b	Cp_{min}	l	α_3	β	$\Delta\beta_{pot}$	C_{Lpot}
0.1	-0.421	0.364	1.402	64.571	2.909	0.296
0.2	-0.436	0.364	0.789	63.958	2.909	0.296
Radial Station e – σ = 0.73, β_3 = 67.105, β_∞ = 68.101, Δβ = 1.913, C_L = 0.245						
C_b	Cp_{min}	l	α_3	β	$\Delta\beta_{pot}$	C_{Lpot}
0.1	-0.393	0.384	0.827	67.932	1.915	0.245
0.2	-0.409	0.384	0.227	67.332	1.915	0.245

In an attempt to evaluate an optimum value for cascade turbine design, from the cascades of the Tab. 3**,** five turbines were built with blades of different geometric characteristics. The constructive geometries of the turbines are presented in Tab. 4. In the designs A and B is verified that the profiles of the radial stations that make up the blade shape present the same curvature . While the designs C, D

and E present a smoothing of the curvature, with profiles close to the hub being the most curved ones. It is also verified that the close region of the hub presents the largest hydrodynamic loading (Tab. 3).

Table4. Constructive geometries of the turbines.

	Design	A	B	C	D	E
	C_b	0,1	0,2-	0,5	1,0	1,2
	Cp_{min}	-4,246	-3,208	-0,713	-0,733	-0,752
	σ	1,210	1,210	1,210	1,210	1,210
	l	0,292	0,292	0,292	0,292	0,292
	α_3	13,290	12,520	9,918	5,848	4,251
	β	47,154	46,384	43,782	39,712	38,115
	$\Delta\beta$	16,195	16,195	16,195	16,712	16,712
i	C_L	0,632	0,632	0,632	0,632	0,632
	Design	A	B	C	D	E
	C_b	0,1	0,2	0,4	0,5	0,5
	Cp_{min}	-0,556	-0,562	-0,580	-0,588	-0,588
	σ	1,000	1,000	1,000	1,000	1,000
	l	0,312	0,312	0,312	0,312	0,312
	α_3	5,822	5,114	3,685	2,967	2,967
	β	54,660	53,952	52,523	51,805	51,805
	$\Delta\beta$	8,293	8,293	8,293	8,293	8,293
1	C_L	0,482	0,482	0,482	0,482	0,482
	Design	A	B	C	D	E
	C_b	0,1	0,2	0,2	0,3	0,3
	Cp_{min}	-0,473	-0,485	-0,485	-0,499	-0,499
	σ	0,870	0,870	0,870	0,870	0,870
	l	0,333	0,333	0,333	0,333	0,333
	α_3	2,823	2,178	2,178	1,528	1,528
	β	60,365	59,720	59,720	59,070	59,070
	$\Delta\beta$	4,711	4,711	4,711	4,711	4,711
2	C_L	0,377	0,377	0,377	0,377	0,377
	Design	A	B	C	D	E
	C_b	0,1	0,2	0,2	0,2	0,2
	Cp_{min}	-0,421	-0,436	-0,436	-0,436	-0,436
	σ	0,800	0,800	0,800	0,800	0,800
	l	0,364	0,364	0,364	0,364	0,364
	α_3	1,402	0,789	0,789	0,789	0,789
	β	64,571	63,958	63,958	63,958	63,958
	$\Delta\beta$	2,908	2,908	2,908	2,908	2,908
3	C_L	0,296	0,296	0,296	0,296	0,296
	Design	A	B	C	D	E
	C_b	0,1	0,2	0,2	0,2	0,2
	Cp_{min}	-0,393	-0,409	-0,409	-0,409	-0,409
	σ	0,730	0,730	0,730	0,730	0,730
	l	0,384	0,384	0,384	0,384	0,384
	α_3	0,827	0,227	0,227	0,227	0,227
	β	67,932	67,332	67,332	67,332	67,332
	$\Delta\beta$	1,913	1,913	1,913	1,913	1,913
e	C_L	0,245	0,245	0,245	0,245	0,245

Numerical Flow Simulation. Results and Discussions

The commercial CFX-TASCflow code, which is specific for solution of flows in turbomachinery and that solves the Navier-Stokes 3D equations in its conservative form, was used as the basis for the flow solution. The simulation domain includes the space between the runner's inlet and outlet, hub and shroud region (Fig. 4).

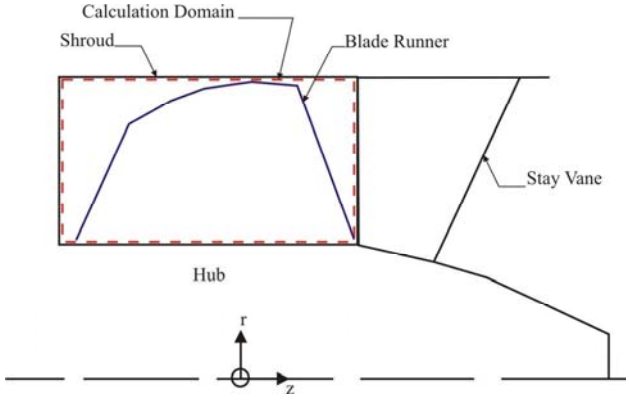

Figure 4. Calculation domain.

The basic dimensions (l and s) for tested channel in relation to the cord of profile are showed in Tab. 5 in function of the stations radial (Fig. 3). They are same for five designs (A, B, C, D, E). The Table 5 also presents the solidity of the channel.

Table 5. Basic dimensions and solidity for tested channel.

	i	1	2	3	e
l (m)	0,292	0,301	0,312	0,320	0,384
s (m)	0,241	0,276	0,312	0,348	0,526
l/s (-)	1,210	1,090	1,000	0,920	0,730

The choose geometry for the cannel of the calculation domain is the NACA 65-series-airfoil. It is very utilized for turbomachines projects that don't have a big load. At that case, there is a big pressure gradient along of the profile. This fact carries a softer flow behavior and easier to be modeled numerically. The geometries of the flow simulation domain were exported for CFX-TURBOgrid for grid generation.

The complete grid consisted of about 30,000 elements. The grid is structured and adapted to periodic geometries of turbomachines blades. It is rectangular (Fig. 5) with a grid aspect ratio equal to 100 as recommended for the software. This one also recommends a minimum intern angle of grid elements bigger or equal to 23°. In this study, the angle is equal to 28°. A mesh refining was provided in the regions close to solids walls to assure a satisfactory simulation of the flow in limit layer. Figure 5 shows the grid in the blade-to-blade plane from CFX-TURBOgrid.

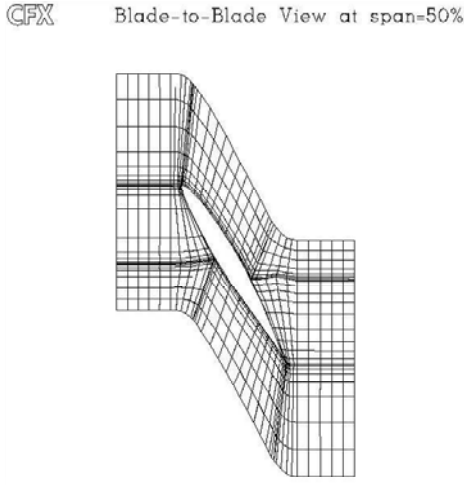

Figure 5. Blade-to-blade plane of the grid view.

Since the geometry of the turbines is rather simple, this number was sufficient in a way that the grid could be adjusted fine enough in the vicinity of the walls that the wall function could be employed to represent the effect of the walls on the flow. Great care was taken to ensure that the log-law value determined by the closest grid points to the wall was below the acceptable limits. Since that parameter is directly related with the treatment of boundary layers close to the solid walls. It is essential since the mechanical power of the turbine was evaluated integrating pressure and wall shear stress distribution on the runner surfaces.

The runner turbines analyzed consists of four blades. For the rotating frame of reference (including runner blade and hub) the boundaries conditions are set as rotating wall condition and the value of the rotating velocity is equal to 53.05 rad/s, a stationary wall condition was forced by default for the absolute frame of reference (shroud) regarded as being smooth and their design is treated by making use of the log-law drawing; inlet condition. For the inlet region of the runner, the boundary condition was specified with the fluid flow velocity directions, $w_r = 0\ m/s$ (radial velocity), $w_u = -10.71\ m/s$ (tangential velocity) and $w_a = 6{,}81\ m/s$ (axial velocity). Outlet condition is characterized for region of small pressure, after turbine runner. Thus, the static pressure scalar field can be increased by a numerical value without affecting the flow solution. The periodic condition is automatically generated by CFX-TASCgrid.

The flow is considered as being incompressible and turbulent. The turbulence model k-ε has been used for validation process with values of k and $\varepsilon = 10^{-4}$. This convergence criteria is also utilized for validation the pressure and velocity fields.

The numeric analyses carried out for the viscous flows aims at evaluating the quality of the design geometries (A, B, C, D and E), seeking to determine, through its hydraulic efficiencies, an optimum value as axial turbines design criterion. These comparative results are presented in Tab. 6.

Table 6. Comparisons of numerical results for the designed runner.

Global Parameters	DESIGN				
	A	B	C	D	E
Specific Energy, E, [J/kg]	42.35	41.73	41.12	43.62	43.08
Total head, H, [m]	4.317	4.254	4.191	4.446	4.392
Torque, T, [N·m]	1250	1249	1258	1317	1293
Flow number, φ_e , [-]	0.302	0.302	0.302	0.302	0.302
Pressure coefficient, ψ_e , [-]	0.269	0.265	0.261	0.277	0.274
Hydraulic power number λ_e ,[-]	0.081	0.080	0.079	0.084	0.083
Velocity coefficient, ν , [-]	1.475	1.488	1.505	1.440	1.453
Torque coefficient, τ_e , [-]	0.068	0.068	0.068	0.071	0.699
Efficiency, η , [-]	0.830	0.840	0.860	0.850	0.846

The hydraulic efficiency and the global parameters were calculated for the nominal operational point with constant rotational speed. Figure 6 shows the hydrodynamic loading along the distribution of the blade of each turbine.

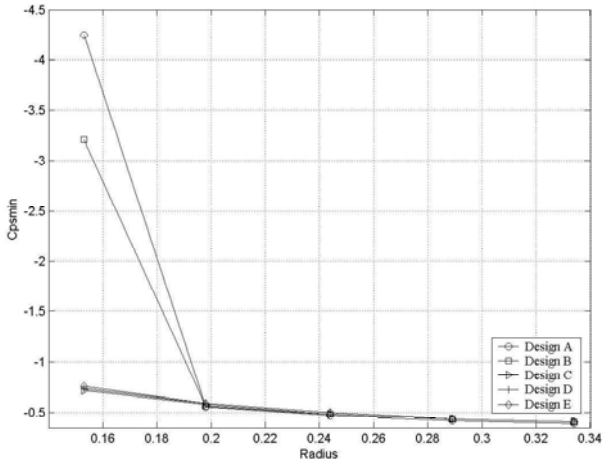

Figure 6. Hydrodynamic loading distribution on the blade.

The diagram of Fig. 7 presents comparison between the hydraulic efficiencies of the runners in relation to the hydrodynamic loading close to the hub.

The maximum efficiency calculated was *86.2* percent, obtained with the turbine C that was designed with minimum suction pressure coefficient in the fixed range design, distributed along the blade runner. The larger hydraulic loading is close to the hub and the smallest in the tip of the blade. The radial station profiles that form the blade runner are a little curved, with camber coefficient between *0.5* (in the hub) to *0.2* (blade's tip).

It is observed that the blades presenting profiles with constant camber in all its extension tend to have a smaller hydraulic efficiency when a high hydrodynamic loading close to the hub is fixed, this is verified in the design A and B. Similar situation is verified in the case of blades built with uniformly distributed hydrodynamic loading and with different camber profiles, presenting lower efficiency for large close curvatures to the hub, this is verified in designs D and E. Design C presents a more uniform distribution of the profile cambers of the radial stations as well as the hydrodynamic loading distribution along the blade presenting greater efficiency.

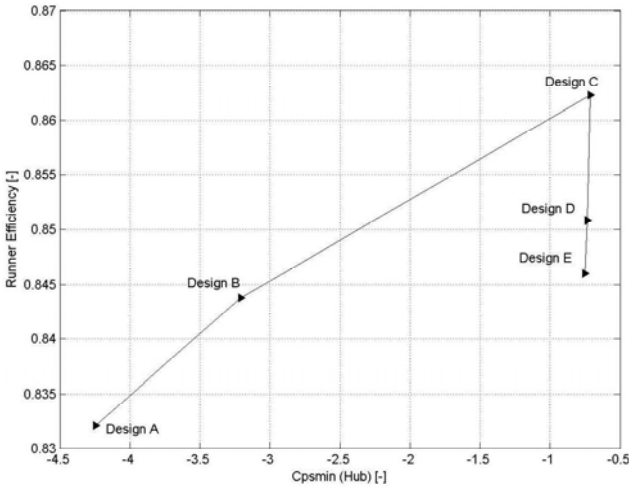

Figure 7. Efficiency compared with the hub hydrodynamic loading.

The visualization of the results obtained for the turbine of better efficiency is made through mid-span surfaces in the blade-to-

blade plane. The velocity vectors, static pressure and relative velocity on the mean surface are shown in Fig. 8, Fig. 9 and Fig. 10, respectively.

The consistency of the numerical simulation can be verified regarding the geometric and hydraulic parameters of the designs carried out. The flow direction is observed on the blades surfaces and the static pressures show regions subject to a larger hydrodynamic loading. This numerical consistence is not sufficient to show the Von Karman's Vortexes in downstream flow (Fig. 8). It is due to mesh refining, which is limited for the memory of personal computer (PC), and turbulence model adopted in the software Navier-Stokes 3-D TASCflow. Thus, a mesh refiner and another turbulence model showed the Von Karman's Vortexes.

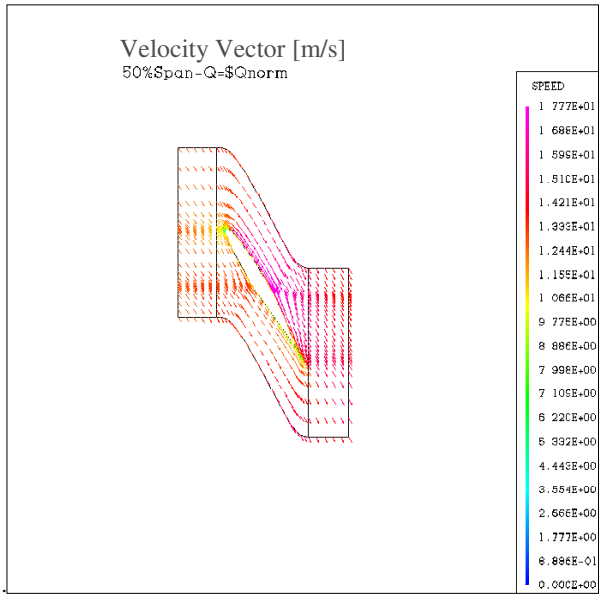

Figure 8. Velocity vectors at mid-span of the turbine.

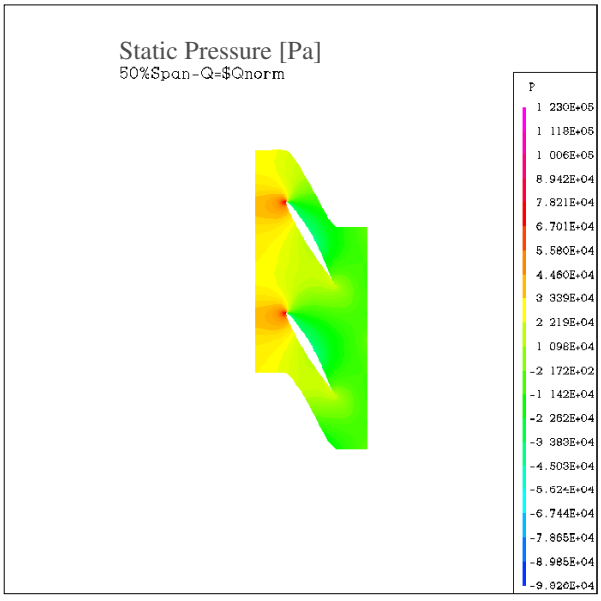

Figure 9. Static Pressure at mid-span of the turbine.

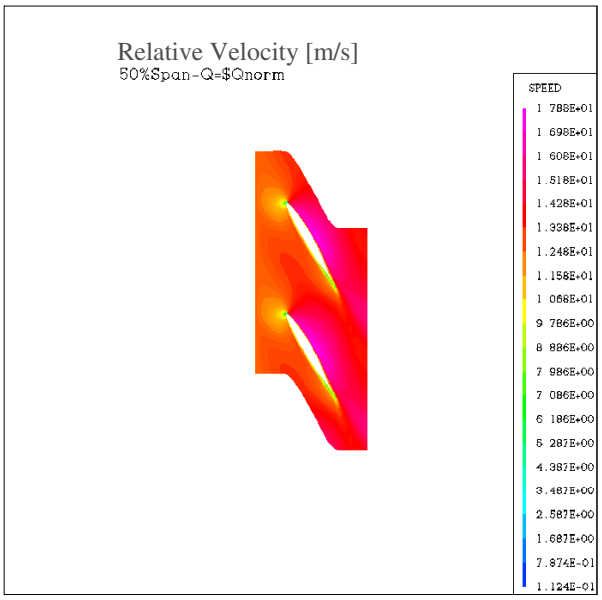

Figure 10. Relative velocity at mid-span of the turbine.

By analyzing the minimum pressure coefficient obtained values and by comparing them with the designs of fans tested by Amarante Mesquita et al. (1996), the result obtained is quite different. For the fans tested, the optimum value established is equal to *-2.0* and in the present work it was concluded that the design value of the C_{pmin} lies within the range of $-0.8 \leq C_{p\,\min} \leq -0.4$, where the greater hydrodynamic loading is close to the hub and the smallest loading in the tip of the blade, uniformly distributed. In the case of a hydraulic turbine, a small loading is required in the tip of the blades, which implicates in its enlargement, from the hub to the shroud, due to prevention of the cavitation risks. Thus, only one design value is not observed, but a range of loading values. Since in the case of fans there is not the danger of the blade cavitation, it can be worked with a constant value of the C_{pmin}. This implicates in a decrease of the blades width, from the hub to shroud.

Conclusion

A study regarding the application of the minimum suction pressure coefficient, C_{psmin}, as a simplified methodology for axial hydraulic turbine was present. The cascade geometric parameters are determined in order to obtain a value that provides the required flow condition, both geometric and hydrodynamic, this analysis was made using an inviscid flow methodology and numeric simulations through the commercial CFX-TASCflow. Five axial hydraulic turbines were designed. The design C presents best hydraulic efficiency. The designs A, B, D, and E have hydraulic efficiency a little smaller than the design C and pressure coefficients slightly bigger than this one. These differences between hydraulic efficiency and pressure coefficient are explained for the profile curvature increase that carry out the secondary flow in the region close to the hub.

Finally, the visualization of scalar fields flow (velocity vectors, static pressure and relative velocity) at the mid-span of the blade channels provides a qualitative validation of the turbine geometry of best hydraulic efficiency can be accomplished.

The presented methodology establishes a range for optimum cascade selection of hydraulic turbine with high efficiency, showing to be a good indication of the determination of an initial geometry of this turbomachine type; however, other comparative studies are

required in order to confirm the proposed values. Other influences must be considered for the improvement of this design methodology such as secondary flows, tip clearance, which were not considered here. Also cavitation effects must be analyzed in more details.

References

AEA Technology Engineering Software Limited, 2000, "CFX-TASCFow" User Documentation Version 2.10, Waterloo, Ontario, Canada.

Cruz, A. G. B., 2002, "A Methodology for Small Axial Hydro Turbine Design" (in Portuguese), M. Sc. Thesis, Universidade Federal do Pará, Belém, Brasil.

Amarante Mesquita, A. L., Manzanares Filho, N. and Fernandes, E. C., 1996, "A Methodology for Axial Flow Turbomachine Design", Proceedings Of the VI ENCIT-LATYCIM, vol. 3, pp. 1883-1886, Florianópolis, Brasil.

Amarante Mesquita, A. L., Cruz, D. O. A., 1999, Serra, C. M. V. and Manzanares Filho, N., "A Simplified Method for Axial-Flow Turbomachinery Design", Journal of the Brazilian Society of Mechanical Sciences, Vol. 21, No. 1, pp. 61-70.

Amorim, J. C. C., 1986, "Potencial Flow Calculation Around Isolated Airfoils and Through Turbomachine Cascades" (in Portuguese), M.Sc Thesis, Escola Federal de Engenharia de Itajubá, Minas Gerais, Brasil.

De La fuente, R. P., 1982, "Performance Evaluation Criteria for Linear Cascade" (in Portuguese), M. Sc. Thesis, Instituto Tecnológico de Aeronáutica, S. J. Campos, Brasil.

De Palma, P., 2006, "Numerical simulations of three-dimensional transitional compressible flows in turbomachinery cascades", International Journal of Numerical Methods for Heat & Fluid Flow, Vol. 16, No. 4, pp. 509-529.

Fernandes, E. C., 1973, " Analysis of the Geometric Parameter Influences on Axial Flow Turbomachine Design" (in Portuguese), M. Sc. Thesis, Instituto Tecnológico de Aeronáutica, S. J. Campos, Brasil.

Gostelow, J. P., 1974, "Cascade Aerodynamics", Pergamon Press, Elmsford, N. Y.

Herrig, L. J., Emery, J. C., Erwin, J. R. e Felix, A. R., 1957, "Systematic Two-Dimensional Cascade Tests of NACA 65 Series Compressor Blades at Low Speeds", NACA TN 3916.

Lewis, R. I, 1991, "Vortex Element Methods for Fluid Dynamic Analysis of Engineering Systems", Cambridge University Press.

Manzanares Filho, N., 1994, "Flow Analysis in Axial-Flow Turbomachines" (in Portuguese), Ph.D. Thesis, Instituto Tecnológico de Aeronáutica, S. J. Campos, Brasil.

Nilsson, H. and Davidson, L., 2003, "Validation of CFD against velocity and pressure measurements in water turbine runner flow", International Journal for Numerical Methods in Fluids, Vol. 41, Issue 8, pp. 863-879.

Raab, J., 1985, "Hydro Power: The Design, Use and Function of Hydro mechanical, Hydraulic and Electrical Equipment", VDI-Verlag GmbH, Düsseldorf, Germany.

Scholz, N., 1965, "Aerodinamik der Scaufelgitter", Band I, Verlag G. Braun, Karlsruhe.

Schweiger, F. and Gregori, J., 1990, "Analysis of Small Hydro Turbine Design", Small Hydro Power.